ELSEVIER

Contents lists available at ScienceDirect

Radiation Measurements

journal homepage: www.elsevier.com/locate/radmeas





Assessing quartz luminescence sensitivity protocols for fine-grained sediments in marine sediment cores

Priscila E. Souza ^{a,*}, André O. Sawakuchi ^b, Dayane B. Melo ^b, Fernanda C.G. Rodrigues ^c, Cristiano M. Chiessi ^c, Stefan Mulitza ^d, Vinícius R. Mendes ^e

- ^a Department of Environmental Sciences, Federal University of São Paulo, Diadema, Brazil
- b Institute of Geosciences, University of São Paulo, São Paulo, Brazil
- ^c School of Arts, Sciences and Humanities, University of São Paulo, São Paulo, Brazil
- ^d MARUM-Center for Marine Environmental Sciences, University of Bremen, Bremen, Germany
- ^e Marine Sciences Institute, Federal University of São Paulo, Santos, São Paulo, Brazil

ARTICLE INFO

Keywords: Luminescence protocols Luminescence sensitivity of silt Sample preparation Palaeoprecipitation proxy

ABSTRACT

Applications of quartz luminescence beyond sediment dating are expanding rapidly. A growing number of studies have successfully applied quartz optically stimulated luminescence (OSL) and thermoluminescence (TL) sensitivities in sediment provenance investigations and palaeoclimate reconstructions based on marine sediment cores, which are usually composed of fine-grained sediments (silt and clay), demanding measurements on polymineral samples. However, the procedures during sample preparation and the luminescence measurement conditions for determining the quartz OSL and TL sensitivities of fine-grained polymineral samples have not yet been extensively assessed. Here, we present the results of five different tests designed to determine whether the current procedures employed when preparing the samples and measuring their quartz luminescence sensitivities could be improved and/or simplified. The tests include assessing the dependency of quartz OSL and TL sensitivities on: (1) luminescence measurement conditions (i.e., with and without preheat, with light stimulation at room temperature and at 125 °C, based on natural and laboratory dose); (2) aliquot mass; (3) number of aliquots per sample; (4) grain size selection; and (5) feldspar content. Tests were performed on polymineral fine sediments from two marine cores. GeoB16206–1 and M78/1-235-1, recovered from the western equatorial Atlantic. close to the mouth of the Parnaíba and Orinoco rivers, respectively. In general, our results show that the procedures when preparing polymineral aliquots for quartz OSL or TL sensitivity measurements can be easily optimized on a case-by-case basis, saving time and resources. Our key result is that quartz OSL sensitivity obtained using natural signals and measured without thermal treatments (Test 1) are very similar to the results obtained using regenerative doses and preheating. This opens the possibility of reducing the OSL measurement time by 70 % and of scanning marine sediment cores with portable luminescence readers without the use of radiation sources for signal regeneration. Tests 2 and 3 show that both OSL and TL sensitivity results given by more than six aliquots or by aliquots made of 0.4 mg to 5 mg are indistinguishable. Waiting longer settling times to subsample finer fractions before mounting the aliquots (Test 4) is helpful to reduce feldspar, but it may also reduce the quartz significantly, limiting the ${\rm \%BOSL_{1s}}$ analysis. Finally, including an etching step to reduce feldspar (Test 5) is a helpful procedure to improve the TL and OSL sensitivity analysis, but not necessarily feasible for routine application with hundreds of samples.

1. Introduction

The quartz optically stimulated luminescence (OSL) and thermoluminescence (TL) sensitivities, i.e., the light emitted per unit mass per radiation dose, is a property that has been in vogue for sediment

provenance studies (e.g., Capaldi et al., 2022; Goswami et al., 2024; Gray et al., 2019; Sawakuchi et al., 2012, 2018, 2020; Souza et al., 2023). Recent investigations have emphasised that the OSL sensitivity of quartz grains is mainly related to processes (e.g., solar exposure and burial irradiation and/or surface heating) affecting quartz in soils of the

E-mail address: pri.emerich97@gmail.com (P.E. Souza).

^{*} Corresponding author.

source areas and, thus, is useful to track sediment provenance (e.g., Capaldi et al., 2022; Magyar et al., 2024; Sawakuchi et al., 2018; Zhang et al., 2023). Variations in the sources of continental sediments supplied to the oceans may be induced by changes in precipitation patterns (e.g., Mulitza et al., 2013; Zhang et al., 2015) and, therefore, the quartz luminescence sensitivity has been shown to be a useful tool for palae-oclimate studies (e.g., Campos et al., 2022; Mendes et al., 2019). Assessing the luminescence sensitivity of quartz grains from marine sediment cores is particularly relevant, because they are widespread across the continental margins and, unlike continental deposits, they are not exposed to post-depositional modifications affecting quartz luminescence.

Specifically, the quartz luminescence sensitivity applied in sediment provenance studies refers to the fast OSL component (Jain et al., 2003), usually measured using blue light stimulation (referred to as "BOSL1s"), and to the 110 °C thermoluminescence signal peak (TL110) (e.g., Pagonis et al., 2002). According to Campos et al. (2022), employing the quartz luminescence sensitivity in marine sediment cores as a proxy for continental precipitation has some advantages over other classic proxies, such as stable hydrogen isotopes in specific molecules and elemental ratios in bulk sediments (e.g., Ti/Ca), because it (i) responds fast to changes in continental precipitation, (ii) lacks post-depositional biases (i.e. dissolution), and (iii) is not influenced by effects related to rainfall isotopic fractionation and changes in relative sea-level or biogenic carbonate production.

Employing the quartz OSL and TL sensitivities of fine sediments recovered from marine cores as palaeoclimate proxies is a novelty (Campos et al., 2022, 2025; Mendes et al., 2019) and, thus, some methodological aspects have not yet been broadly appraised. In the pioneer work by Mendes et al. (2019), and then in Campos et al. (2022), the procedures to prepare the polymineral samples for luminescence measurements included chemical treatments with hydrogen peroxide and hydrochloric acid to eliminate organic matter and carbonate minerals, respectively, and making a solution by adding alcohol/acetone to the remaining sediment until 5 mL; after homogenised, three aliquots (discs) per sample were prepared by adding four drops of the solution on luminescence measurement discs (Mendes et al., 2019). In that study, however, the amount of material (given the number of solution drops) used to mount each disc (aliquot), the necessary number (n) of aliquots per sample, and the grain size selection have not been systematically evaluated.

Regarding the luminescence measurement conditions, OSL and TL sensitivities are usually calculated from signals obtained using regenerative doses after preheating, and with hot optical stimulation, in case of OSL sensitivity measurements (e.g., Liu et al., 2022; Mendes et al., 2019; Sawakuchi et al., 2018; Zhang et al., 2023). OSL measurements usually include such thermal treatments (i.e., preheating and hot optical stimulation) to avoid contamination from the peak-shaped isothermal TL signal in the OSL (Murray and Wintle, 2003), increasing the fast-to-slow components ratio (Jain et al., 2003). Studies have demonstrated that the unstable signals coming from medium and slow components may also be sensitized (e.g., Moska and Murray, 2006; Tsukamoto et al., 2011) and, thus, are potentially useful. However, in case of polymineralic samples, the presence of feldspar would interfere in the analysis, making it difficult to distinguish the signals from medium and slow components. Sawakuchi et al. (2020) have conducted tests varying preheating and stimulation temperatures for measuring the quartz OSL sensitivity of sediments from various geologic contexts, but these tests were performed with pure quartz aliquots in the sand grain size ((150–250) $\mu m)$ and the OSL signals derived from regenerative doses. They have also measured silt samples from marine sediment core GeoB16206-1 collected offshore northeastern Brazil (also used in this study), however they have neither measured TL sensitivity nor investigated the OSL sensitivity of signals derived from natural doses or any different procedures when preparing the aliquots (Sawakuchi et al., 2020).

Here, we aim at broadening the tests performed by Sawakuchi et al. (2020) on silt grain size samples, which dominate marine or lacustrine sediment cores collected for palaeoclimate investigations. Simplifying the procedures to assess quartz luminescence sensitivity of fine-grained sediments, keeping the reliability and significance of the results, would be a substantial contribution to the scientific community engaged in using quartz OSL and TL sensitivities in sediment provenance and palaeoclimate investigations. A simpler preparation and faster reading protocol could significantly decrease the time necessary to prepare and analyse samples, allowing higher resolution luminescence studies from sediment cores.

Five tests are presented in this study, each one exploring a different aspect of the sample and/or aliquot preparation (Table 1): (1) luminescence measurement conditions; (2) aliquot mass; (3) number of aliquots per sample; (4) grain size selection; and (5) feldspar concentration. Test 1 aims at verifying if/how the sensitivity from a natural OSL signal (i.e., acquired during burial irradiation) measured without preheating and stimulated at room temperature (blue OSL at 20 °C) correlates to a signal derived from regenerative dose, with preheating and hot blue light stimulation (blue OSL at 125 $^{\circ}$ C). Tests 2 and 3 aim at, respectively, verifying the quartz OSL and TL sensitivity dependency on aliquot mass and determining how many aliquots per sample are sufficient to obtain reproducible results. Test 4 aim at assessing the quartz OSL and TL sensitivity dependency on grain size selection. Finally, Test 5 includes treatment with hydrofluoric acid (HF) to a sample of low quartz luminescence sensitivity and/or high feldspar content to reduce feldspar concentration and, thus, increase the proportion of quartz OSL signal. The results of these five tests are presented and discussed in light of other quartz luminescence sensitivity data obtained from protocols of published studies in similar sediment cores retrieved from the Brazilian continental margin (e.g., Campos et al., 2022; Mendes et al., 2019; Sawakuchi et al., 2018, 2020).

2. Materials and methods

Given the strong methodological aspect of this work and to facilitate the reading, only general information that applies to all tests will be presented in this section. Details on the materials and methods employed in each test will be presented in dedicated sections along with respective results and discussions. A summary of all tests specificities is provided in Table 1.

2.1. Studied marine sediment cores

Tests were performed using fine-grained (silt) polymineral sediments from two marine sediment cores, namely GeoB16206-1 (Mulitza et al., 2013) and M78/1-235-1 (Bahr et al., 2018). The first four tests were performed using the samples from GeoB16206-1, while the fifth test was performed with a sample from M78/1-235-1 (Table 1). In all cases, the sample code represents the depth of the sample within the core to which a modelled age is associated (Nürnberg et al., 2021; Zhang et al., 2015).

Both marine sediment cores studied here comprehend a mixture of marine biogenic and continental terrigenous sediments delivered by South American rivers. GeoB16206-1 was retrieved from the northeastern Brazilian continental slope (1°34.75′ S, 43°01.42′ W) at a water depth of 1367 m (Supplementary Fig. S1) during cruise MSM20/3 (AMADEUS; Mulitza et al., 2013). The most important river delivering sediments to this area is the Parnaíba River (Supplementary Fig. S1) (Zhang et al., 2015). The sediments (continental terrigenous and marine biogenic clasts) of GeoB16206-1 have already been extensively studied and reported in previous studies (e.g. Campos et al., 2022; Portilho-Ramos et al., 2017; Zhang et al., 2015), including the study by Mendes et al. (2019) and Sawakuchi et al. (2020) who have also investigated its quartz luminescence sensitivity. In fact, core GeoB16206-1 was selected because it has already been studied using "conventional protocols" to measure the quartz OSL and TL sensitivities (Mendes et al., 2019) and,

Table 1– Summary of all tests performed in this study, where: *aliquot n* indicates the number of aliquots (discs) mounted for each sample; *drop n* makes reference to the number (quantity) of drops of the solution with sediment and alcohol that make each aliquot; %BOSL_{1s} represents the quartz optically stimulated luminescence (OSL) sensitivity given as the percentage of the contribution of blue OSL fast component (BOSL_[1s]) to the other more slowly decaying components (see section 2.5).

#	Test identification	Core	Aliquot n	Drop n	Signal type	Thermal treatment	Test purpose
1	Luminescence Measurement conditions	GeoB16206- 1	3	5	Natural	No	To check whether natural signals measured at room temperature and without thermal treatment can yield %BOSL _{1s} values comparable to those obtained from regenerated OSL signals measured with thermal treatments
2	Aliquot mass	GeoB16206- 1	3	1 to 10	Regenerated	Yes	To check the dependency of $\mathrm{\%BOSL_{1s}}$ and $\mathrm{\%TL_{110}}$ to the size (mass) of the aliquot
3	Number of aliquots	GeoB16206- 1	10	5	Regenerated	Yes	To check how many aliquots per sample are sufficient to obtain reproducible results
4	Grain size dependence	GeoB16206- 1	3	5	Regenerated	Yes	To check the dependency of mean of $\mbox{\rm \%BOSL}_{1s}$ and $\mbox{\rm \%TL}_{110}$ to grain size selection
5	Feldspar concentration	M78/1-235	6	5	Regenerated	Yes	To check whether the $\rm \%BOSL_{1s}$ and $\rm \%TL_{110}$ could be improved by removing/reducing the interference of feldspars

thus, our results could be compared to theirs. By "conventional protocols" we mean calculating the OSL sensitivity from regenerated signals, after a preheating and with light stimulation at 125 °C. The geochronological framework for this marine sediment core is based on radiocarbon ages from planktonic foraminifera (Zhang et al., 2015). Here, we updated the original age model by employing a more recent radiocarbon calibration curve (IntCal20, Reimer et al., 2020) and a local marine reservoir correction derived from model experiments (Butzin et al., 2020; Heaton et al., 2020) as implemented in the software Pale-oDataView (Langner and Mulitza, 2019) (Supplementary Fig. S2).

Piston core M78/1-235-1 was retrieved off Trinidad (11°36.53′ N, 60°57.86′ W) at a water depth of 852.2 m during cruise 78/1 (Schönfeld et al., 2012). This area is under the influence of the Orinoco River discharge (Supplementary Fig. S1), the third-largest drainage basin in South America. The age model used was published by Nürnberg et al. (2021), who has updated and extended the chronostratigraphy initially published by Hoffmann et al. (2014) and Poggemann et al. (2017, 2018). Preliminary (screening) tests have shown that the sediments delivered by the Orinoco River are characterized by low luminescence sensitivity quartz and relatively high content of feldspar, which makes it a good case to include in our tests for improving samples preparation and measurement protocols.

Bulk samples from GeoB16206-1 were collected at the University of Bremen (Germany) and stored in the Luminescence and Gamma Spectrometry Laboratory (LEGAL) at the Institute of Geosciences of the University of São Paulo (IGc-USP, Brazil). M78/1–235 samples were collected at GEOMAR, Kiel (Germany), and stored at LEGAL. All samples were processed and measured at LEGAL.

2.2. Luminescence measurements

Table 2 presents the protocols applied for the luminescence measurements in Test 1 (left column) and the Tests 2 to 5 (right column). Infrared stimulated luminescence (IRSL), detected through ultraviolet (UV) filters, was used before OSL to reduce feldspar luminescence with minor influence on quartz OSL (Wallinga et al., 2002).

All luminescence measurements were carried out using a Risø TL/OSL DA-20 reader in the LEGAL facilities. The reader is equipped with $a^{90} Sr/^{90} Y$ beta source, delivering a dose rate of $\sim\!0.075$ Gy/s, blue ((470 \pm 20) nm, maximum power of 80 mW/cm²) and infrared (870 nm, maximum power of 145 mW/cm²) LEDs for stimulation, and Hoya U-340 filter for light detection in the UV band (290 nm–340 nm).

2.3. Luminescence sensitivities calculation

Following Sawakuchi et al. (2018), the OSL sensitivity was calculated in relative terms as expressed in Equation (1):

Table 2

– Optically stimulated luminescence (OSL) and thermoluminescence (TL) sensitivities measurement sequences employed in Test 1 (left-hand column) and tests 2 to 5 (right-hand column). Infrared stimulated luminescence (IRSL) is used to presumably deplete the luminescence emitted by feldspar grains. The dose size given (steps 3 and 8) was test-specific: 15 Gy in tests 1 to 4, and 50 Gy in test 5. Note that the main difference between both sequences shown in the left-hand and right-hand columns is that in the left-hand column, there is no quartz bleaching step at the beginning of the sequence, and the measurements of the hatural dose signal are made at room temperature. Steps assigned with an index "b" correspond to measurements run for appraising the remnant signal used for background calculation of the previous measurement.

Step	Treatment for Test 1	Treatment for tests 2 to 5
1	IRSL at 20 °C for 100 s	IRSL at 125 °C for 100 s (bleaching)
2	OSL at 20 °C for 100 s ($Ln_{20^{\circ}C}$)	OSL at 125 °C for 100 s (bleaching)
2b	OSL at 20 °C for 100 s (background)	
3	Beta irradiation (15 Gy)	Beta irradiation (15 or 50 Gy)
4	TL at 200 °C for 10 s, 5 °C per s	TL at 200 °C for 10 s, 5 °C per s
	(preheating)	(preheating)
5	IRSL at 125 °C for 100 s	IRSL at 125 °C for 100 s
6	OSL at 125 °C for 100 s (Lx _{125°C})	OSL at 125 °C for 100 s
6b	OSL at 125 °C for 100 s	OSL at 125 °C for 100 s
	(background)	(background)
7	TL at 250 °C for 0 s, 5 °C per s	TL at 250 $^{\circ}$ C for 0 s, 5 $^{\circ}$ C per s
8	Beta irradiation (15 Gy)	Beta irradiation (15 or 50 Gy)
9	TL at 250 °C for 0 s, 5 °C per s	TL at 250 °C for 0 s, 5 °C per s
9b	TL at 250 °C for 0 s, 5 °C per s	TL at 250 °C for 0 s, 5 °C per s
	(background)	(background)

$$\%BOLS_{1s} = \frac{BOSL_{[0:1\ s]} - BG_{[0:1\ s]}}{BOSL_{[0:100\ s]} - BG_{[0:100\ s]}}$$
(Equation 1)

Where $BOSL_{[0:1\ s]}$ and $BOSL_{[0:100\ s]}$ correspond, respectively, to the integral of the first second and of the total OSL curve recorded in step 6 (Table 2). Similarly, $BG_{[0:1\ s]}$ and $BG_{[0:100\ s]}$ correspond to the integrals of the respective intervals but from the OSL curve recorded in step 6b (Table 2), a measure of the signal background. This calculation yields an OSL sensitivity relative value (%), hereafter termed %BOSL_{1s}, which corresponds to a signal dominated by the fast OSL component, assuming the first second of light emission as dominated by the fast OSL component, in relation to the medium and slow components. This approach aims to reduce instrumental influence on luminescence sensitivity estimates, which is needed for intercomparison of data obtained by different luminescence readers.

Similarly, TL relative sensitivity (%) was obtained by the ratio of the integral of a temperature interval around the so-called 110 $^{\circ}$ C TL peak, minus the respective background, to the integral of the total curve, minus the respective background (Equation (2)). Since the 110 $^{\circ}$ C TL peak was observed to occur below 110 $^{\circ}$ C, the integration limit comprehended the curve area from 50 $^{\circ}$ C to 100 $^{\circ}$ C. The background (BG in

Equation (2)) was obtained from the TL curve measured in step 9b (Table 2, left-hand column), in which the signal had been depleted in the previous step. Hereafter, such TL relative sensitivity is termed $\%TL_{110}$.

$$\%TL_{110} = \frac{TL_{[50:100\ ^{\circ}C]} - BG_{[50:100\ ^{\circ}C]}}{TL_{[0:250\ ^{\circ}C]} - BG_{[0:250\ ^{\circ}C]}}$$
 (Equation 2)

3. Test 1: luminescence measurement conditions

In Test 1, 28 light-protected samples (i.e., having the natural luminescence signal preserved) were selected from core GeoB16206-1, covering the last 30,000 years. For each sample, approximately 0.5 g of sediment was weighted and put into a 50 mL Falcon tube. They were subjected to chemical treatment using oxygen peroxide (H₂O₂) 35 % and hydrochloric acid (HCl) 40 % to remove organic matter and carbonates, respectively. Between the acidic treatments, samples were washed with distilled water (and centrifuged) until the reagents were completely removed. Alcohol (70 %) was added until 10 mL to the remaining material to make a solution, which was homogenised and left to rest for 18 s before a sub-sample was collected at depth of \sim 1 cm using a disposable pipette. When necessary, the homogenisation was facilitated by putting the tubes in an ultrasonic cleaner for a few minutes (to deflocculate the sample). Using the disposable pipette, a drop (~0.05 mL) at a time was dripped on each disc until completing five drops - i.e., one drop was added to each disc, then the second, then the third, then the fourth, and finally the fifth. In test 1, three aliquots per sample, making 28 in total, were mounted on luminescence discs (Table 1). We opted for heating these discs up to 40 °C on a hot plate to speed up the liquid (alcohol) evaporation. That interval of 18 s was given by Stokes' Law and ensures that we sub-sampled in the range of interest only, i.e., <63 µm. Unlike all other tests, all procedures in Test 1 were performed under subdued orange light to preserve the sample natural dose.

The luminescence measurements for Test 1 followed the protocol presented in Table 2, left column. The aliquots, which had their natural dose preserved, were first stimulated with IRSL at room temperature (20 $^{\circ}$ C) for 100 s to reduce the feldspar signals (step 1). Then, they were stimulated twice with blue OSL at room temperature for 100 s to measure the natural quartz OSL signal ($Ln_{20^{\circ}C}$, step 2) and its respective background (step 2b). Next, a known dose of 15 Gy was administered (step 3), aliquots were preheated to 200 °C for 10 s (step 4), and we repeated the IRSL (step 5) and OSL stimulations (steps 6 and 6b) but, this time, at 125 °C. Finally, aliquots were heated to 250 °C as a clean out, a dose of 15 Gy was given, and a TL stimulation at 250 °C was employed twice to register the TL glow curves given by 15 Gy (step 9) and 0 Gy (i. e., background; step 9b). The data given step 2 (and 2b) corresponds to the signal used to calculate the OSL sensitivity of Ln_{20°C}: a signal given by a natural dose, measured at room temperature, and without any preheating treatment. The data given in step 6 (and 6b) corresponds to the signal used to calculate the OSL sensitivity of Lx_{125°C}: a signal given by a laboratory dose, preheated to 200 °C, and stimulated at 125 °C.

OSL sensitivities were calculated based on Equation (1). Additionally, we calculated ratios between the IRSL and OSL data (IRSL $_{[1s]}$) BOSL $_{[1s]}$), which give information on the feldspar content. The IRSL intensity (IRSL $_{[1s]}$) was given by the integral of the first second of the IRSL stimulation curve, minus a late background (last 10 s of the curve). Test 1 results were normalised in order to compare our results to those published by Mendes et al. (2019) and Sawakuchi et al. (2020), who investigated the same sediment core used in this test (i.e., GeoB16206-1). We used the Z-score normalisation, obtained by subtracting from each value the mean and dividing it by the standard deviation of the dataset.

3.1. Test 1: results and discussion

BOSL counts in the first second of the light stimulation given by each approach were different, with $Ln_{20^{\circ}C}$ yielding twice as many counts as

the Lx_{125°C} (Fig. 1A). Such difference in the absolute number of counts is not surprising, as they derived from doses of different sizes – natural and unknown dose, which varied from sample to sample, against a fixed regenerative dose of 15 Gy. The %BOSL_{1s} values, in turn, were notably similar (Fig. 1C; Table S1) and showed significant positive correlation (r = 0.86, α = 0.05; Fig. 2). %BOSL_{1s} mean values ($\pm 1\sigma$) derived from Ln_{20°C} and Lx_{125°C} signals ranged from (9 \pm 2) % to (38 \pm 11) % and from (8.9 \pm 0.5) % to (25 \pm 4) %, respectively (Fig. 1C and Fig. 2; Table S1).

The $IRSL_{[1s]}/BOSL_{[1s]}$ data given by $Ln_{20^{\circ}C}$ and $Lx_{125^{\circ}C}$ signals were also very similar to each other (Fig. 1D). Noteworthy is the relation between $\%BOSL_{1s}$ and $IRSL_{[1s]}/BOSL_{[1s]}$ data: decreasing mean $\%BOSL_{1s}$ values were accompanied by an increasing trend of the $IRSL_{[1s]}/BOSL_{[1s]}$ ratio (e.g., see in Fig. 1C and D the trend from depth \sim 350 cm towards the core top), when the feldspar contribution increases (Fig. 1B, from 350 cm to 0 cm). Were this correlation positive, i.e., with $IRSL_{[1s]}/BOSL_{[1s]}$ and BOSL increasing/decreasing in the same direction, it would be an indication that the OSL signal is not coming from quartz but is dominated by feldspar. In case of polymineral samples characterized by low quartz sensitivity and high content of feldspar, other procedures would be necessary to see quartz OSL signal, such as thermal sensitization, pulsed OSL, or acid treatments for example.

The normalised data shown in Fig. 3, performed to allow data intercomparison, make it even more evident that quartz OSL sensitivity from natural signals measured at room temperature and without preheating agree with those derived from signals of regenerative doses measured with thermal treatments. Moreover, the results given by $Ln_{20^{\circ}C}$ (this study) are also in line to those reported by Sawakuchi et al. (2020), who investigated the role of thermal treatments on quartz OSL sensitivity measurements using samples from the same core as in this study (i.e., GeoB16206-1) but employing a regenerative dose ($Lx_{20^{\circ}C}$, 10 Gy) (Fig. 3B).

Some variation in the calculated %BOSL1s data among these approaches was expected because of fundamental differences among natural and laboratory irradiations (e.g., Peng et al., 2022), mainly under different thermal treatments (e.g., Wang et al., 2021; Murray and Wintle, 1998). OSL signals from natural doses are less affected by the preheating treatments because, in fact, they already have a smaller contribution of medium and slow components, which are more unstable and, thus, naturally fade through time. In the case of OSL signals from regenerative doses, the time between irradiation and light stimulation often used (<300 s) is not sufficiently long to allow the fading of the unstable components and, therefore, the preheating is employed prior to the light stimulation to essentially remove them (Jain et al., 2007). Such removal of unstable components through artificial heating is efficient, but not as efficient as the fading in nature. For instance, Wang et al. (2021) have reported on how differently natural and regenerated OSL signals of fine-grained quartz may respond to the same thermal treatment and how these differences may affect the equivalent dose (ED) estimation for OSL dating. They showed that quartz OSL sensitivity of signals from regenerative doses (Lx signals) are much more affected by variations in the preheat temperature than the signals from natural doses (Ln signals), resulting in ED (and so age) underestimation (Wang et al., 2021). Here, however, these differences between natural and regenerative dose signals and their response to preheating did not seem to affect the analysis outcome, for both Ln_{20°C} and Lx_{125°C} signals provided results (OSL sensitivity) that point in the same direction. Moreover, it is noteworthy that no difference nor pattern in the %BOSL_{1s} data error bars behaviour was observed: $Ln_{20^{\circ}C}$ data did not necessarily yield larger relative standard errors than the respective $Lx_{125^{\circ}C}$ data (Table S1). One could expect to see this systematic difference in the error bars, because of intra-sample dose differences: the natural dose in each aliquot for the same depth is expected to be similar but may not be the same, whereas the regenerative (laboratory) dose is the same. Our observation reinforces that the relative luminescence sensitivity is not dependent on dose size.

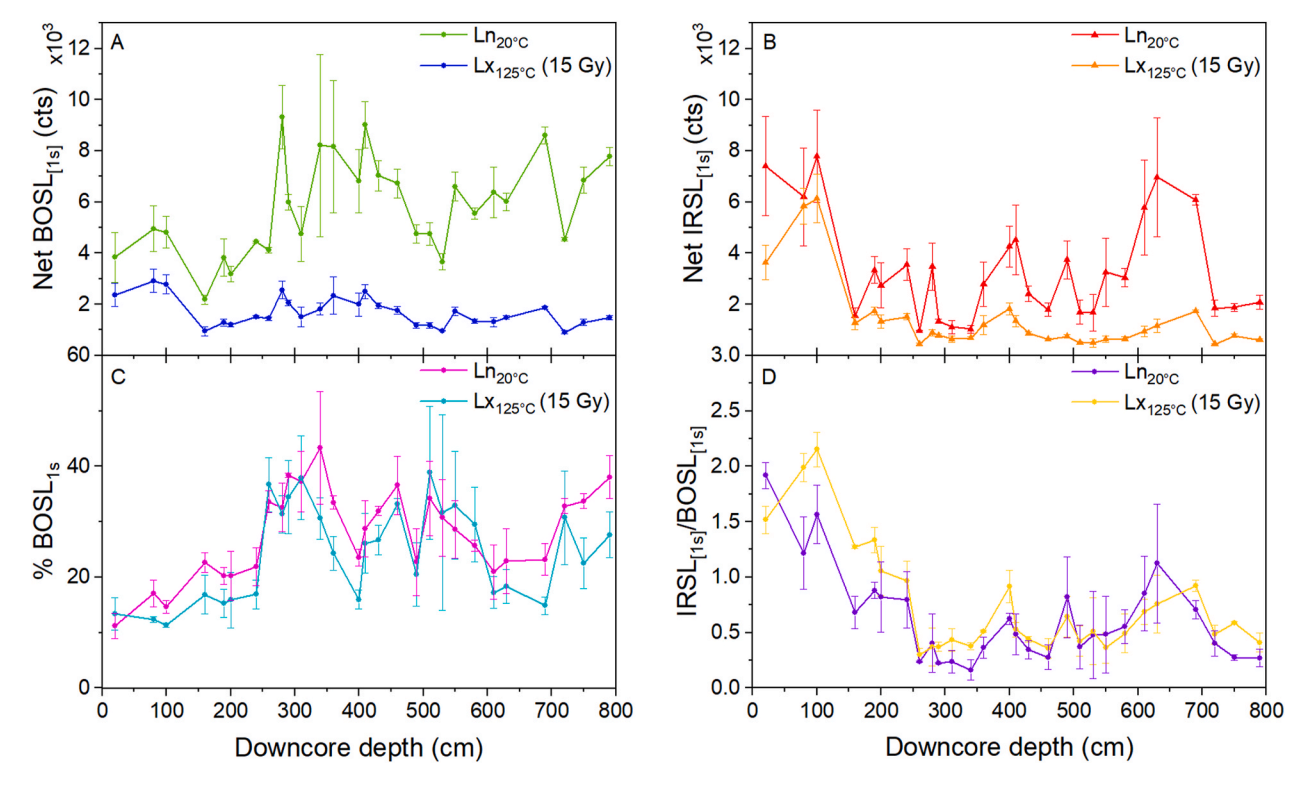


Fig. 1. – Test 1 results. Two data set are shown in all plots: $Ln_{20^{\circ}C}$ and $Lx_{125^{\circ}C}$. The former, $Ln_{20^{\circ}C}$, was given by the sample natural dose, stimulated at room temperature and without preheating, while $Lx_{125^{\circ}C}$ data was obtained from a regenerative dose (15 Gy), stimulated at 125 °C, after preheating. A and B show the sum of photon counts (background subtracted) emitted in the first second blue/infrared stimulations, per sample/depth. C and D show, respectively, quartz OSL relative sensitivities (%BOSL_{1s}) and $IRSL_{[1s]}/BOSL_{[1s]}$ ratios. In all graphs, each point represents the mean (\pm standard error) of three aliquots. Note that the y-axes in A and B are multiplied by 10^3 . (For interpretation of the references to colour in this figure legend, the reader is referred to the Web version of this article.)

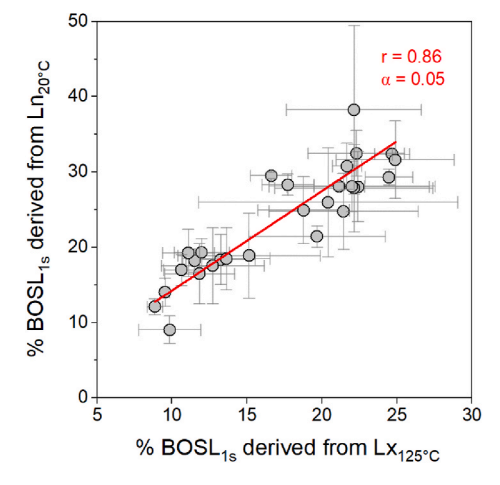


Fig. 2. – Correlation between %BOSL $_{1s}$ data obtained from natural and regenerated (15 Gy) OSL signals measured, respectively, at room temperature without preheating (Ln $_{20^{\circ}\text{C}}$) and at 125 °C after a preheating of 200 °C (Lx $_{125^{\circ}\text{C}}$).

Test 1 results suggest that both natural and laboratory signals yield % BOSL_{1s} with similar range and precision. Such conclusions are encouraging, for they open the possibility of making fast measurements directly on core samples using portable luminescence readers, such as other measurements (e.g., gamma density, magnetic susceptibility, X-ray fluorescence, etc.) are already routinely performed using multisensor core loggers. A drawback, however, could be making measurements in bulk samples (in contrast to what was used in this study and by Sawakuchi et al. (2020)). One could argue that if the measurements of this study had been performed with bulk samples (i.e., if organic matter and

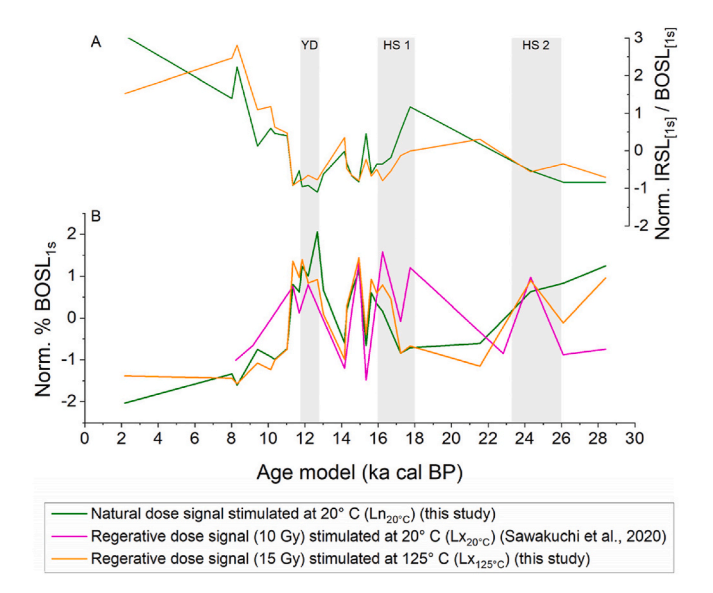


Fig. 3. – Normalised luminescence sensitivity data of samples from marine sediment core GeoB16206-1 obtained in Test 1 (green and orange curves), and the data (magenta curve) compiled from Sawakuchi et al. (2020). While panel (A) shows $IRSL_{[1s]}/BOSL_{[1s]}$, panel (B) depicts %BOSL_{1s}, both normalised. Green and magenta curves show OSL signals of natural dose ($In_{20^{\circ}C_i}$; this study) and of regenerative dose (10 Gy, $Ix_{20^{\circ}C_i}$; Sawakuchi et al., 2020), respectively, both stimulated at room temperature without preheating. The orange curve shows the OSL regenerated signals stimulated at 125 °C, after preheating at 200 °C (15 Gy, $Ix_{125^{\circ}C_i}$; this study). Gray-shaded areas indicate the period of the events Heinrich stadials (HS1 and HS2) and Younger Dryas (YD). (For interpretation of the references to colour in this figure legend, the reader is referred to the Web version of this article.)

carbonates had not been removed), the natural signals measured at room temperature (Ln_{20°C}) would not yield sensitivity results similar to those from regenerative dose measured in the presence of thermal treatments (Lx_{125°C}). To address that, a preliminary test was performed using some light-exposed bulk samples from GeoB16206-1 that were still available and had been investigated by Mendes et al. (2019) and by Sawakuchi et al. (2020). %BOSL_{1s} results from Lx_{125°C} signals of bulk versus treated samples showed satisfactory correlation (r = 0.76, Supplementary Fig. S3A) and followed the same trend as those from Lx_{20°C} obtained by Sawakuchi et al. (2020) (Supplementary Fig. S3B). Thus, the results obtained in Test 1 (Ln_{20°C}, Lx_{20°C}, Lx_{125°C}, and Lx_{125°C} from treated and bulk samples) were satisfactorily similar. They all provide information for palaeoclimate interpretation in the same direction as reported by Mendes et al. (2019): higher %BOSL1s values during the climate events Heinrich stadials (HS1 and HS2) and Younger Dryas (YD), which are characterized by enhanced precipitation, followed by a gradual decrease in %BOSL1s along the Holocene (Fig. 3B).

4. Test 2: aliquot mass

Test 2 was performed using a sample from GeoB16206-1, the same as in Tests 3 and 4. In these tests (2 to 4), there was no need to select a sample whose natural signal was still preserved and, thus, the selected representative sample was that with (i) the higher amount of bulk material still available and (ii) the higher quartz signal sensitivity given in previous/preliminary measurements. Following the criteria above, the selected sample was from the downcore depth 490 cm of core GeoB16206-1.

The selected sample was prepared in the same manner as that in Test 1 (i.e., weighting to \sim 0.5 g, treating with H₂O₂ 35 % and HCl 40 %, and making a solution with alcohol), however aliquots were mounted differently. Here, we used the same sample (i.e., same core (GeoB16206-1), same depth (490 cm)) to prepare 30 discs varying from one to ten drops every three discs, which makes three aliquots per number of drops. Therefore, in this case, "sample 1" corresponds to aliquots prepared with one drop of the solution, "sample 2" with two drops, and so on until getting to the tenth sample prepared with ten drops per disc. For samples with more than five drops, it was necessary to wait until the solution on the disc (aliquot) had evaporated to add the remaining drop. Finally, these discs were weighted with and without the sample after being measured (on the luminescence reader) to determine each aliquot's mass. Mean weights (\pm standard deviation, n = 3) of the aliquots according to the number of drops (1 to 10) added to the discs were the following: (0.42 \pm 0.07) mg, (0.84 \pm 0.10) mg, (1.34 \pm 0.10) mg, (1.69 \pm 0.06) mg, (2.29 \pm 0.04) mg, (2.92 \pm 0.12) mg, (3.37 \pm 0.42) mg, (3.75 \pm 0.08) mg, (4.98 \pm 0.48) mg, and (5.2 \pm 1.01) mg.

The luminescence measurements in Test 2 employed the protocol shown in Table 2, right column, which is similar to that used to measure $Lx_{125^{\circ}C}$ signals in Test 1. The difference is that, here, the aliquots were bleached using IRSL and OSL stimulations at 125 °C for 100 s.

4.1. Test 2: results and discussion

In Test 2, the dependency of $\%BOSL_{1s}$ and $\%TL_{110}$ on aliquot mass was assessed. Results are summarised in Fig. 4, which shows the mean values calculated for $\%BOSL_{1s}$ and TL_{110} sensitivity obtained for aliquots of 0.4 mg to 5.2 mg. The data did not show any clear trend with the increase in the mass of the aliquots (Fig. 4). Most samples fell within the mean values of (18.6 \pm 2.18) % and (26.0 \pm 3.20) % for $\%BOSL_{1s}$ and TL_{110} sensitivity, respectively (Fig. 4).

Test 2 results were encouraging, for it was observed no dependency (nor trend) of ${\rm \%BOSL_{1s}}$ on the aliquot mass – no dependency for the considered interval of 0.4 mg to 5.2 mg, at least. It means that a standardized aliquot preparation procedure is enough for reliable (relative) sensitivity measurements in fine-grained sediments, dismissing the need for adopting a more laborious procedure that include weighting each

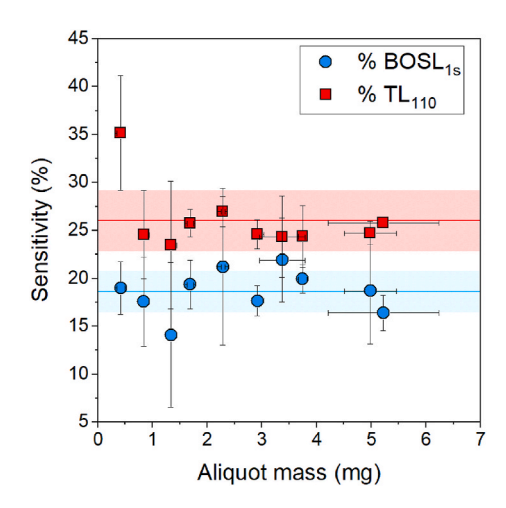


Fig. 4. – Test 2 results. The y-axis shows the sensitivity values for $\%BOSL_{1s}$ (blue circles) and $\%TL_{110}$ (red squares) data. Each symbol represents the mean \pm 1σ of three aliquots made using the same quantity of drops (1–10). The blue and red horizontal solid lines and shaded areas indicate the average of all % $BOSL_{1s}$ and $\%TL_{110}$ data, respectively (shaded areas correspond to 1σ). (For interpretation of the references to colour in this figure legend, the reader is referred to the Web version of this article.)

disc to calculate absolute sensitivity values (i.e., in $\operatorname{cts} \cdot \operatorname{Gy}^{-1} \cdot \operatorname{mg}^{-1}$). For this sample (GeoB16206-1, depth 490 cm), to which was given a laboratory dose of 15 Gy, an aliquot with a mass as low as 0.5 mg is enough to yield reliable and reproducible %BOSL_{1s} and %TL₁₁₀ values. Consistency is probably what matters the most, i.e., to use the same measure (drops quantity) for all aliquots of the same sediment core. Since there is no trend and aliquots made of, for instance, 4 or 9 drops yield similar results, there is no need to spend effort and material mounting discs with more grains; 4 drops (1.7 mg) are enough.

5. Test 3: number of aliquots

Test 3 was performed with aliquots made with the sample of core GeoB16206-1 at the depth 490 cm (i.e., the same as in Tests 2 and 4). The sample preparation followed those in the previous tests (i.e., same acid treatments and general manner to prepare the aliquots), but we prepared ten aliquots with five solution drops each (Table 1).

The luminescence measurement conditions were the same used in the previous test, Test 2 (Table 2, right column).

5.1. Test 3: results and discussion

Here, mean %BOSL $_{1s}$ and %TL $_{110}$ values were calculated using 3, 6, 9, 12, 15, 18, 21, and 24 aliquots. In general, the mean values varied within error limits with the changing number of aliquots: %BOSL $_{1s}$ ranged from (13.5 \pm 3.5) % to (16.6 \pm 2.6) %, and the %TL $_{110}$ ranged from (29.0 \pm 3.3) % to (31.2 \pm 6.6) % (Fig. 5). The most expressive variation was observed for %BOSL $_{1s}$ and %TL $_{110}$ mean values as the numbers of aliquots increased from 3 to 6. In fact, results given by more than six aliquots are indistinguishable (Fig. 5). As for the data dispersion, the larger the number of aliquots, the smaller the relative standard deviation: from three to 24 aliquots, relative standard errors decreased from 26 % to 16 % for %BOSL $_{1s}$, and from 21 % to 12 % for %TL $_{110}$.

Test 3 showed that measuring few aliquots can provide good enough results. Our results demonstrate that, for fine-grained samples, six aliquots are sufficient to yield quartz $\%BOSL_{1s}$ and $\%TL_{110}$ values comparable to as if 24 aliquots were used (Fig. 5). This is probably because aliquots mounted with silt contain a large number of grains compared to sand grains aliquots, which averages the results (Duller, 2008). Obviously, error bars become smaller if more aliquots are employed and, whenever possible, it is preferable to work with smaller uncertainties.

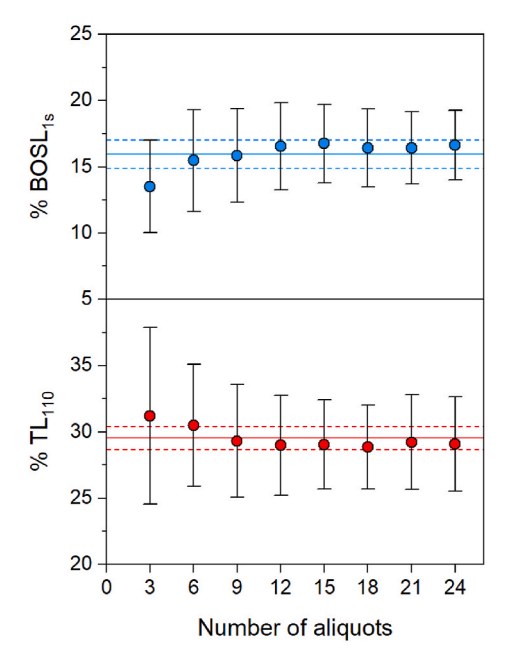


Fig. 5. – Summary of Test 3 results. Symbols correspond to mean values calculated using varying number of aliquots (3 to 24, x-axis). The error bars are given by 1σ . Solid and dashed horizontal lines represent, respectively, the average and \pm 1σ of all points.

However, making more aliquots increases the time of luminescence measurements, which may be a limiting factor in many circumstances. Given the simplicity of the Tests 2 and 3, we recommend performing them prior to sensitivity measurements to ensure that the best choice is made for each set of samples. These tests could be used in the same way the preheat plateau and the dose recovery tests are used for OSL dating

using SAR protocol (Murray and Wintle, 2000).

6. Test 4: grain size dependence

The sample used in this test was the same as in Tests 2 and 3, i.e., from core GeoB16206-1 at 490 cm and, except when mounting the aliquots, the sample preparation (chemical treatment) was the same as in Test 2 and 3. Here, samples rested for different time intervals (18, 60, 120, 180, 240, and 300 s) before sub-sampling and mounting the aliquots (3 per settling time, with five solution drops each) to assess the effect of grain size in measured quartz OSL and TL sensitivities (Table 1). Given that the solution column was of 2 cm and that it was sub-sampled at a depth of 1 cm, the expected grain sizes after 18, 60, 120, 180, 240, and 300 s were, respectively: $<34~\mu m$, $<19~\mu m$, $<13~\mu m$, $<11~\mu m$, $<9.5~\mu m$, and $<8.5~\mu m$.

The luminescence measurements in Test 4 employed the protocol shown in Table 2, right column (same as Tests 2 and 3). For Test 4, however, the intensity of the IRSL signal (IRSL_[1s]) obtained for each sediment settling time was also calculated to investigate the behaviour of the feldspar signal with the change in grain size.

6.1. Test 4: results and discussion

Results obtained in Test 4 show that mean IRSL $_{[1s]}$ values decrease from (530 \pm 92) cts to (46 \pm 16) cts as the aliquots grain size decreases from <34 μ m to <8.5 μ m (Fig. 6A). The solution volume (i.e., number of drops) used to mount these aliquots was the same, however the aliquot mass varies, since finer grains were preferably subsampled with longer settling times. The given dose was the same (i.e., 15 Gy). As shown in Fig. 6A, the most expressive change was observed from settling time 18 s to 120 s, and the mean IRSL $_{[1s]}$ did not change significantly in settling times higher than 120 s.

As for the ${\rm \%BOSL_{1s}}$ data, we could confidently calculate the sensitivity only for the first two settling time intervals, i.e., with aliquots

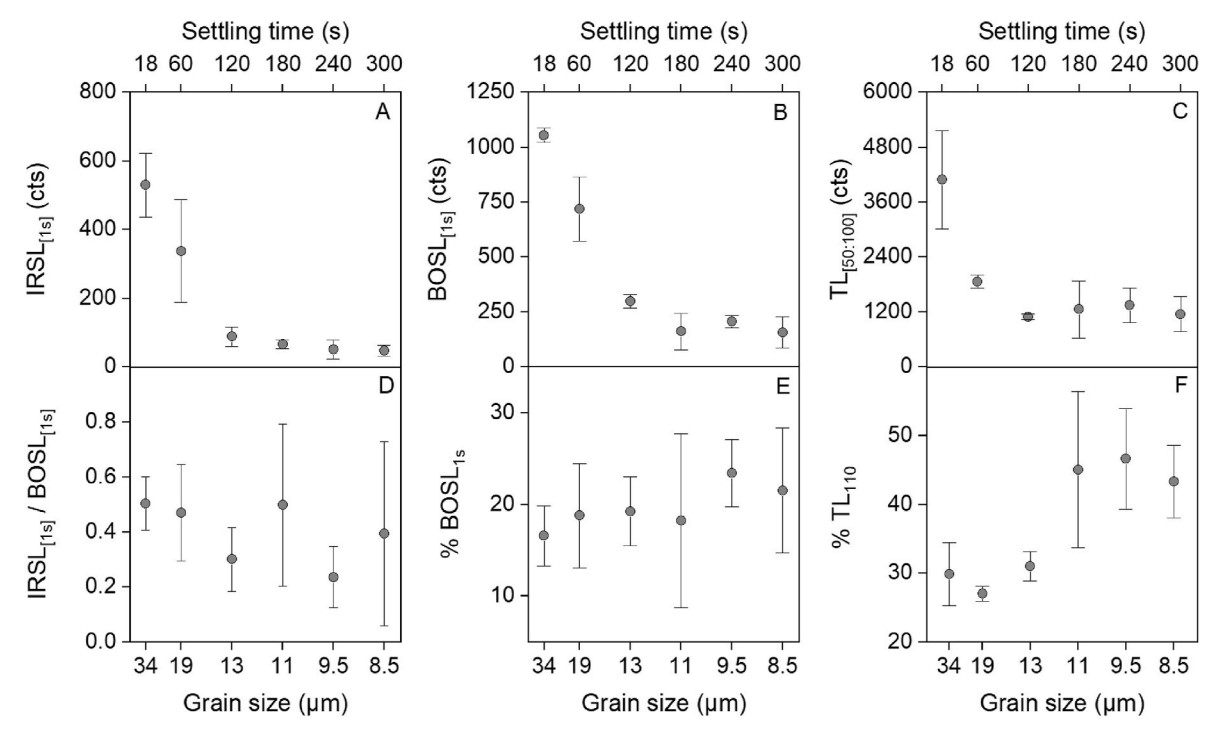


Fig. 6. – Results from Test 4 (grain size dependence): luminescence data as a function of varying settling time and, therefore, of different grain sizes. Panels (A), (B) and (C) show, respectively, the net $IRSL_{[1s]}$, $BOSL_{[1s]}$ and $TL_{[50:100\ c]}$ signals intensity, in counts, plotted against time (top x-axis) waited before mounting the aliquots, and the respective grain sizes (bottom x-axis) expected for each settling time interval. Similarly, panels D, E and F show the ratios between $IRSL_{[1s]}$ and $BOSL_{[1s]}$ data (D), and the relative sensitivities from quartz BOSL (E) and TL (F) signals obtained after different settling times. Each data point corresponds to the mean of three aliquots \pm standard error.

made of grains coarser than 13 $\mu m.$ OSL signals recovered after longer intervals (>120 s) were either slightly above or at the background level (Fig. 6B), which may jeopardize the %BOSL1s results (Fig. 6E). It is likely that the amount of quartz and feldspar grains left after longer intervals (<13 μm) was too small to detect.

The %TL₁₁₀ data suggests an increasing trend of the quartz proportion towards aliquots made of finer grains. There was little variation ((30 \pm 4) % to (31 \pm 2) %) among aliquots made with grains of 34 to 13 µm; however, the mean %TL $_{110}$ increased from (30 \pm 2) % to (45 \pm 11) % and remained at this level for aliquots made of grains $<11 \mu m$ (Fig. 6F). Respective glow curves confirm a change in the TL curves shape as settling times became longer and aliquots were composed of finer grains (Fig. 7). For the first three grain size ranges ($<34 \, \mu m, <19 \, \mu m,$ and $<13 \,$ μm), the quartz TL curves did not show a typical pure-quartz TL $_{110}$ peak, i.e., a curve that increases from a background level, peaks near 110 °C (here \sim 90 °C), and then returns to the background level. Instead, after the peak near 90 $^{\circ}$ C, these TL curves slowly decreased and did not reach the background level (Fig. 7). In the case of the aliquots made with grains ${<}11~\mu m$, the ${TL}_{110}$ peak was better defined (lower panels in Fig. 7), although less intense (i.e., with fewer counts; see Fig. 6C and insets in Fig. 7).

In Test 4, we attempted to see how the quartz sensitivity varies for different grain sizes of the same sample, which were obtained by increasing the settling time before mounting the aliquots on the stainless discs. The rationale is that the proportion of feldspar in the aliquots made of finer fractions may be smaller because they are more susceptible to the weathering process and, thus, may have been dissolved or transformed in autogenic clay minerals. As we go for longer settling times, the amount of material in the aliquot is too small and there is a large intra-sample variation, which may limit the data analysis to some extent. The results shown in Fig. 7 make it clear that both feldspar and quartz signals are significantly reduced after settling time intervals $>\!120$ s (aliquots $<\!13$ μ m). The $'8\!BOSL_{1s}$ values of aliquots made of grains $<\!13$ μ m are too low (near the background level) and, thus, they rather better not be taken at face values but be qualitatively interpreted

as "low sensitivity" or even "dim" signals.

The large errors reflect the fact that the longer the settling time, the more difficult it is to prepare even aliquots (at least, manually). If the large error bars are ignored for a moment, the data seem to suggest that after 60 s (grain sizes <19 μ m) it is possible to recover slightly larger % BOSL_{1s} mean values than when in the presence of "larger" grains (Fig. 6E), possibly because the proportion of quartz increases. In fact, the mean IRSL_[1s] values decrease from 18 s to 60 s (Fig. 6A), indicating less feldspar contribution in the later. The effect of decreasing feldspar content in aliquots made of finer grains is also evident in the TL data, which show an increasing mean %TL110 as settling time increases (Fig. 6F) and an improvement in the TL curves shape (Fig. 7). Note that it is only after settling times >120 s that the TL₁₁₀ quartz peak is better distinguishable and not followed by a plateau that could be related to the feldspar TL signal (Fig. 7). We conclude that working with finer grains is an efficient way to remove the contribution from feldspar, mainly from TL signals. However, the fact that the OSL counts become too low in aliquots made after longer settling time (>120 s) limits this strategy as a means to minimize the feldspar contribution to improve the %BOSL_{1s} data, because most quartz is also being eliminated. In this case, mounting larger aliquots (increasing the amount of material) may be helpful.

7. Test 5: feldspar concentration

Unlike the other tests, Test 5 was performed using four representative samples selected from M78/1-235-1 core at depths at 118 cm, 128 cm, 133 cm and 253 cm. Three aliquots per sample were prepared using the same chemical treatments (H_2O_2 and HCl) and manner as the previous tests (settling time = 18 s, n drops in each aliquot = 5). Then, the samples were subjected to an additional step with hydrofluoric acid (HF) to eliminate or, at least, minimize the feldspar content in the sample. HF 40 % was administered to the samples and left to rest still for 1 h and 40 min. Supernatants were discarded, samples were washed with distilled water and centrifuged until completely removing the reagent. Solutions

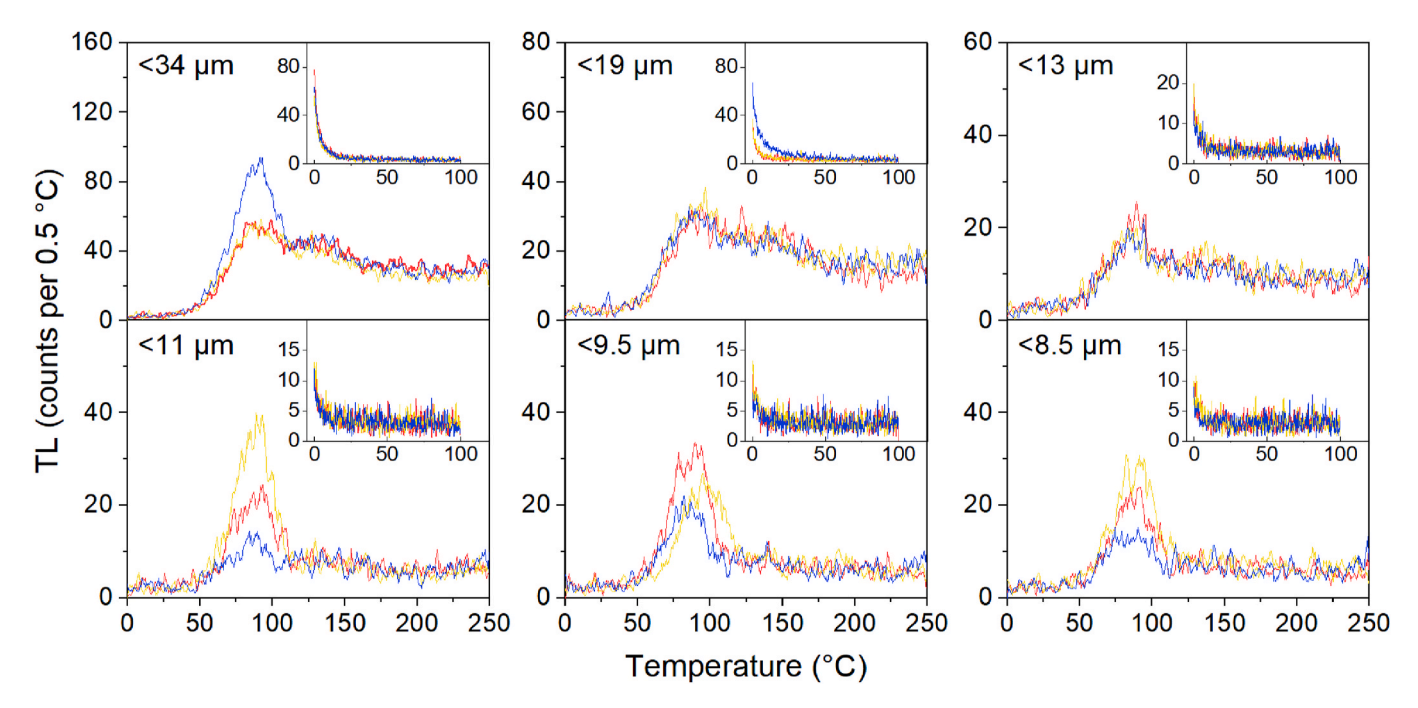


Fig. 7. – Test 4 TL and IRSL (inset) curves from all aliquots and for each expected grain size range (i.e., $<34 \,\mu\text{m}$, $<19 \,\mu\text{m}$, $<13 \,\mu\text{m}$, $<11 \,\mu\text{m}$, $<9.5 \,\mu\text{m}$, and $<8.5 \,\mu\text{m}$) given the different employed settling times (i.e., $18 \, \text{s}$, $60 \, \text{s}$, $120 \, \text{s}$, $180 \, \text{s}$, $240 \, \text{s}$, and $300 \, \text{s}$). Each curve corresponds to an aliquot made of grains in the size range indicated in the graph top right corner. Insets show the respective IRSL curves. Note that the colours of the curves are only used to distinguish them – e.g., the black curve in panel " $<34 \,\mu\text{m}$ " is not related to any other black curve; also, to facilitate the data visualization, y-axes are not in the same scale. (For interpretation of the references to colour in this figure legend, the reader is referred to the Web version of this article.)

with alcohol and the remaining HF-treated sediments were then prepared, homogenised, left to rest for 18 s, and subsampled in the same manner as in the previous tests. Again, three aliquots per sample, with 5 drops of the solution each, were prepared. Therefore, in Test 5, we prepared six aliquots per sample: three without HF attack and three after HF attack.

The luminescence measurement followed the same protocol as in Tests 2 to 4 (Table 2, right column), however the given dose in Test 5 was higher: 50 Gy.

7.1. Test 5: results and discussion

OSL, TL, and IRSL curves obtained in Test 5 with samples from core M78/1-235-1 showed that employing an HF treatment to fine grained polymineral samples was effective to improve all signals for quartz sensitivity measurement purposes (Fig. 8B and D). In general, aliquots treated with HF yield OSL decay curves with less counts (\sim 50 % less intense, Fig. 8A vs B), however there is an improvement in %BOSL1s values (Fig. 9A, Table S2). For instance, in the case of the sample representing the depth 253 cm, the quartz OSL signals of two (out of three) aliquots not treated with HF were not sufficiently above the background level (i.e., they were smaller than two times the background plus 3 σ); therefore, they were on the edge for calculating %BOSL1s values (Table S2). In contrast, all aliquots of sample "253 cm" subjected to HF yielded an OSL signal sufficiently above the background that could be used to calculate the %BOSL1s (Table S2).

TL curves of aliquots not treated with HF were characterised by a growing signal following the so-called TL_{110} peak (Fig. 8C) and, thus, the area used for $\%TL_{110}$ calculations included these higher values (counts) following "the peak". These counts are not related to quartz, but were included in the $\%TL_{110}$ calculation. Following the HF treatment, the quartz TL_{110} peak became clearly distinguishable (Fig. 8D), i.e., followed by decreasing counts, resulting in less counts but quartz-related TL (Table S2). Consequently, the $\%TL_{110}$ was improved by adding the HF step (Fig. 9B).

As for the IRSL signals, they were almost completely removed from

aliquots treated with HF. On average, the IRSL signals of aliquots treated with HF were 82 % lower than those not treated (Fig. 8E vs F, Table S2). Accordingly, the IRSL $_{[1s]}$ /BOSL $_{[1s]}$ ratio in aliquots subjected to HF treatment was significantly smaller (Fig. 9C and Table S2).

Finally, the results from the test in which HF was employed (i.e., Test 5) were also positive, showing a significant improvement in the data after the acid treatment, as suggest in Prasad (2000). Although the HF treatment causes a loss of both quartz and feldspar, feldspar dissolves more effectively than quartz, increasing the relative proportion of the later. Moreover, removing most of the feldspar reduces the background in the subsequent OSL measurement, which helps better distinguish the OSL signal and allows calculating its sensitivity (as observed in the case of sample 253 cm, Table S2). This would be useful in sediment samples hosting quartz grains with lower OSL and TL sensitivities.

In cases where the feldspar content is relatively high and/or the quartz sensitivity is low, as it is the case of the samples from core M78/1–235, including an HF attack may be the best approach, better than increasing the settling time at least.

8. Conclusions

We tested different ways to prepare samples/aliquots for quartz OSL and TL sensitivity measurements, aiming at simplifying or improving the preparation steps for routine measurements in marine sediments. We specifically worked with polymineral fine-grained sediments obtained from two marine sediment cores collected in the western equatorial Atlantic offshore the mouth of large rivers in sites accumulating from terrigenous sediments.

Our tests show that natural OSL signals measured at room temperature yield quartz OSL relative sensitivity values (i.e., ${\rm \%BOSL_{1s}}$) comparable to those derived from regenerated signals with preheating and hot stimulation. Such finding is encouraging as it shows the possibility of speeding the measurements and of obtaining ${\rm \%BOSL_{1s}}$ values using readers designed for core scanning. Usually, an OSL measurement for sensitivity calculation of only one aliquot takes 20 min or more, depending on the size of the regenerative dose and on the preheating

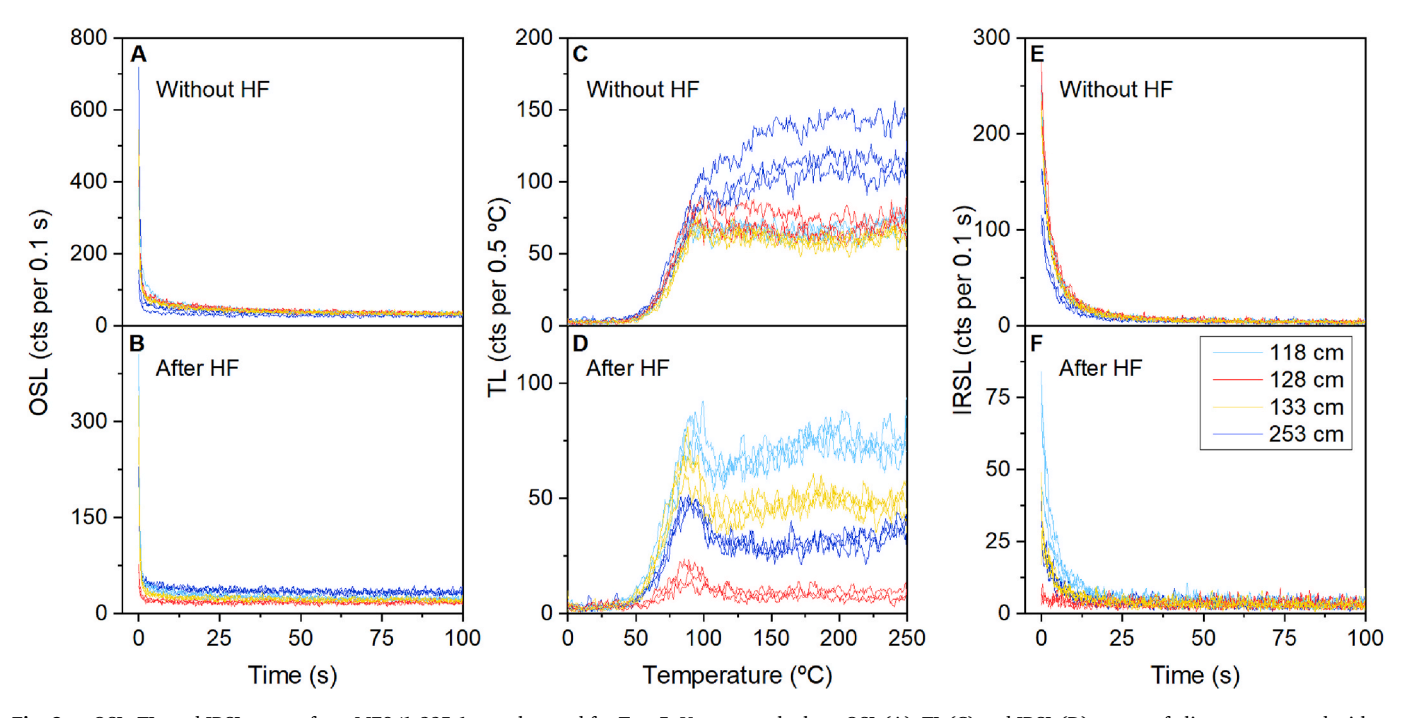


Fig. 8. OSL, TL, and IRSL curves from M78/1-235-1 samples used for Test 5. Upper panels show OSL (A), TL (C) and IRSL (D) curves of aliquots measured without HF treatment, whereas bottom panels (B, D, and F) show the respective curves from aliquots that were subjected to HF treatment prior to measurements. Three curves per colour are presented in each graph as they represent the three aliquots measured per sample (i.e., core depth). Note that y-axes are not in the same scale to facilitate data visualization. (For interpretation of the references to colour in this figure legend, the reader is referred to the Web version of this article.)

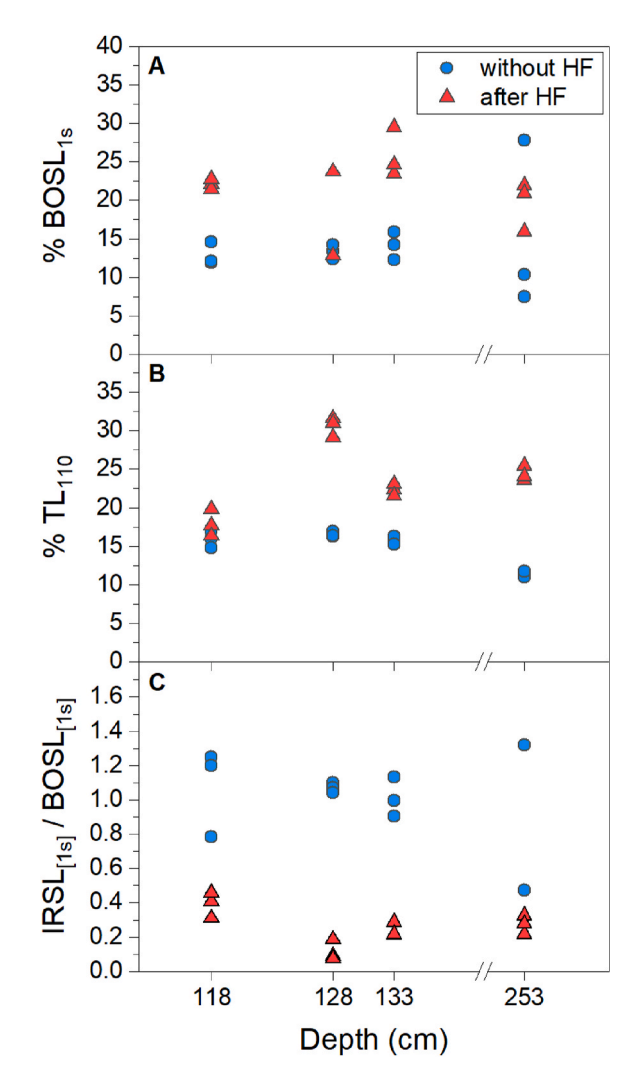


Fig. 9. – (A) %BOSL $_{1s}$, (B) %TL $_{110}$, and (C) IRSL $_{[1s]}$ /BOSL $_{[1s]}$ data obtained from M78-1-235 samples (at depths 118 cm, 128 cm, 133 cm, and 253 cm) for three aliquots prepared without HF treatment (blue circles) and for three aliquots prepared after HF attack (red triangles). (For interpretation of the references to colour in this figure legend, the reader is referred to the Web version of this article.)

employed. However, if the natural dose is measured without any heating, the measurement time of one aliquot is reduced by $70\,\%$ and dismisses the use of an irradiation source.

Moreover, our tests show that the amount of fine-grained sediment on the measurement discs does not affect the $\%BOSL_{1s}$ and $\%TL_{110}$ results. The aliquots' mass was varied by an order of magnitude, but the mean sensitivity values varied within errors. Increasing the number of aliquots does not necessarily improve the results either: six or 24 aliquots yielded indistinguishable results in this study. The ideal amount of material on the disc and the number of aliquots enough to provide reliable results may vary among samples. Therefore, similarly to a preheat plateau test that is routinely performed prior to OSL dating, we recommend including these simple and straightforward tests to a representative sample before performing luminescence sensitivity measurements in a batch of samples. These tests save time, effort, and material when mounting the aliquots.

In the case of fine-grained polymineral samples of characteristically low quartz sensitivity and/or high feldspar content, increasing the settling times before mounting the aliquot to work with finer grains reduced the contribution from feldspar signals, improving the shape of the TL curve. The $\%BOSL_{1s}$ was not as improved as the TL because the

intensity of the BOSL signal was too low (near the background level) in the aliquots made of grains ${<}13~\mu m$ (probably because of the very limited amount of quartz left).

Finally, adding an HF treatment step in sample preparation improved both ${\rm \%BOSL_{1s}}$ and ${\rm \%TL_{110}}$ results by significantly reducing the feldspar content. Such approach, however, is more laborious and may not be feasible for routine application in studies with tens to hundreds of samples, which is common when working with core samples.

CRediT authorship contribution statement

Priscila E. Souza: Writing – original draft, Methodology, Investigation, Formal analysis, Data curation, Conceptualization. André O. Sawakuchi: Writing – review & editing, Supervision, Formal analysis, Conceptualization. Dayane B. Melo: Methodology, Data curation. Fernanda C.G. Rodrigues: Writing – review & editing, Formal analysis. Cristiano M. Chiessi: Writing – review & editing, Formal analysis. Stefan Mulitza: Writing – review & editing, Data curation. Vinícius R. Mendes: Writing – review & editing, Supervision, Resources, Project administration, Funding acquisition, Conceptualization.

Declaration of competing interest

The authors declare that they have no known competing financial interests or personal relationships that could have appeared to influence the work reported in this paper.

Acknowledgements

This work was developed during the post-doctoral research of the first author who was supported by Instituto Serrapilheira under the project ACT ASAP (Grant R-2012-38252) coordinated by VRM. PES acknowledges the São Paulo Research Foundation (FAPESP), Brazil, for the financial support of the current post-doctoral research (2021/ 14022-2). VRM thanks FAPESP (grant 2022/02957-0). AOS thanks the financial support by FAPESP (Trans-Amazon Drilling Project, grants 2018/238899-2 and 2022/08025-1) and the National Council for Scientific and Technological Development (CNPq, Brazil) (grant 307179/ 2021-4). FCGR thanks FAPESP (2022/05520-1 and 2023/15448-9). This study was financed, in part, by FAPESP, processes number 2018/ 15123-4 and 2019/24349-9. CMC acknowledges the financial support from CNPq (grant 312458/2020-7) and CAPES COFECUB, Brazil (grants 8881.712022/2022-1 and 49558SM). D.B.M. thanks FAPESP (2023/15362-7). We thank Prof. Dr. Dirk Nürnberg (GEOMAR, Germany) and Dr. André Bahr (Universität Heidelberg, Germany) for providing the samples from core M78/1-235-1. We thank the captain, crew, and shipboard scientific crew of R/V METEOR cruise M78 for their support. Cruise M78 was funded by the German Science Foundation (DFG) under project 194018713. We are thankful for Dr. Thays D. Maneli's assistance in the laboratory work developed at LEGAL, Brazil.

Appendix A. Supplementary data

Supplementary data to this article can be found online at https://doi.org/10.1016/j.radmeas.2025.107490.

Data availability

Data will be made available on request.

References

Bahr, A., Hoffmann, J., Schönfeld, J., Schmidt, M.W., Nürnberg, D., Batenburg, S.J., Voigt, S., 2018. Low-latitude expressions of high-latitude forcing during Heinrich stadial 1 and the younger Dryas in northern South America. Global Planet. Change 160, 1–9. https://doi.org/10.1016/j.gloplacha.2017.11.008.

- Butzin, M., Heaton, T.J., Köhler, P., Lohmann, G., 2020. A short note on marine reservoir age simulations used in IntCal20. Radiocarbon 62, 865–871. https://doi.org/ 10.1017/RDC.2020.9.
- Campos, M.C., Chiessi, C.M., Novello, V.F., Crivellari, S., Campos, J.L., Albuquerque, A. L., Mendes, V.R., 2022. South American precipitation dipole forced by interhemispheric temperature gradient. Sci. Rep. 12, 10527. https://doi.org/10.1038/s41598-022-14495-1.
- Campos, M.C., Chiessi, C.M., Nascimento, R.A., Kraft, L., Radionovskaya, S., Skinner, L., et al., 2025. Millennial-to centennial-scale Atlantic ITCZ swings during the penultimate deglaciation. Quat. Sci. Rev. 348, 109095.
- Capaldi, T.N., Rittenour, T., Nelson, M.S., 2022. Downstream changes in quartz OSL sensitivity in modern river sand reflects sediment source variability: case studies from Rocky Mountain and Andean rivers. Quat. Geochronol. 71, 101317. https://doi.org/10.1016/j.quageo.2022.101317.
- Duller, G.A., 2008. Single-grain optical dating of Quaternary sediments: why aliquot size matters in luminescence dating. Boreas 37, 589–612. https://doi.org/10.1111/ i.1502-3885.2008.00051.x.
- Goswami, K., Panda, S.K., Alappat, L., Chauhan, N., 2024. Luminescence for sedimentary provenance quantification in river basins: a methodological advancement. Quat. Geochronol. 79, 101488. https://doi.org/10.1016/j.quageo.2023.101488.
- Gray, H.J., Jain, M., Sawakuchi, A.O., Mahan, S.A., Tucker, G.E., 2019. Luminescence as a sediment tracer and provenance tool. Rev. Geophys. https://doi.org/10.1029/ 2019RG000646.
- Heaton, T.J., Köhler, P., Butzin, M., Bard, E., Reimer, R.W., Austin, W.E., Skinner, L.C., 2020. Marine20—the marine radiocarbon age calibration curve (0–55,000 cal BP). Radiocarbon 62 (4), 779–820. https://doi.org/10.1017/RDC.2020.68.
- Hoffmann, J., Bahr, A., Voigt, S., Schönfeld, J., Nürnberg, D., Rethemeyer, J., 2014. Disentangling abrupt deglacial hydrological changes in northern South America: insolation versus oceanic forcing. Geology 42, 579–582. https://doi.org/10.1130/ G35562.1.
- Jain, M., Murray, A.S., Bøtter-Jensen, L., 2003. Characterisation of blue-light stimulated luminescence components in different quartz samples: implications for dose measurement. Radiat. Meas. 37 (4–5), 441–449. https://doi.org/10.1016/S1350-4487(03)00052-0.
- Jain, M., Bøtter-Jensen, L., Murray, A.S., Essery, R., 2007. A peak structure in isothermal luminescence signals in quartz: origin and implications. J. Lumin. 127 (2), 678–688.
- Langner, M., Mulitza, S., 2019. Technical note: PaleoDataView a software toolbox for the collection, homogenization and visualization of marine proxy data. Clim. Past 15, 2067–2072. https://doi.org/10.5194/cp-15-2067-2019.
- Liu, L., Yang, S., Liu, X., Li, P., Wang, H., Zhou, J., 2022. Variation of luminescence sensitivity of quartz grains from loess in eastern Tibetan Plateau and its provenance significance. Front. Earth Sci. 10, 939638. https://doi.org/10.3389/ feart_2022_939638.
- Magyar, G., Bartyik, T., Marković, R.S., Filyó, D., Kiss, T., Marković, S.B., Sipos, G., 2024.
 Downstream change of luminescence sensitivity in sedimentary quartz and the rearrangement of optically stimulated luminescence (OSL) components along two large rivers. Quat. Geochronol. 85, 101629. https://doi.org/10.1016/j.guagep. 2024 101629
- Mendes, V.R., Sawakuchi, A.O., Chiessi, C.M., Giannini, P.C., Rehfeld, K., Mulitza, S., 2019. Thermoluminescence and optically stimulated luminescence measured in marine sediments indicate precipitation changes over northeastern Brazil. Paleoceanogr. Paleoclimatol. 34, 1476–1486. https://doi.org/10.1029/ 2019PA003691.
- Moska, P., Murray, A.S., 2006. Stability of the quartz fast-component in insensitive samples. Radiat. Meas. 41, 878–885. https://doi.org/10.1016/j. radmeas 2006.06.005.
- Mulitza, S., Chiessi, C.M., Cruz, A.P., Frederichs, T., Gomes, J.G., Gurgel, M.H., Wiers, S., 2013. Response of amazon sedimentation to deforestation, land use and climate variability cruise No. MSM20/3 february 19 march 11, 2012 recife (Brazil) bridgetown (Barbados). Bremen: DFG-Senatskommission für Ozeanographie. https://doi.org/10.2312/cr_msm20_3.
- Murray, A.S., Wintle, A.G., 1998. Factors controlling the shape of the OSL decay curve in quartz. Radiat. Meas. 29, 65–79. https://doi.org/10.1016/S1350-4487(97)00207-2.
- Murray, A.S., Wintle, A.G., 2000. Luminescence dating of quartz using an improved single-aliquot regenerative-dose protocol. Radiat. Meas. 32, 57–73. https://doi.org/ 10.1016/S1350-4487(99)00253-X.

- Murray, A.S., Wintle, A.G., 2003. The single aliquot regenerative dose protocol: potential for improvements in reliability. Radiat. Meas. 37, 377–381. https://doi.org/ 10.1016/S1350-4487(03)00053-2.
- Nürnberg, D., Riff, T., Bahr, A., Karas, C., Meier, K.J., Lippold, J., 2021. Age and Sediment Reflectance of Sediment Core M78/1_235-1. https://doi.org/10.1594/PA NGAEA.929961.
- Pagonis, V., Tatsis, E., Kitis, G., Drupieski, C., 2002. Search for common characteristics in the glow curves of quartz of various origins. Radiat. Protect. Dosim. 100, 373–376. https://doi.org/10.1093/oxfordjournals.rpd.a005892.
- Peng, J., Wang, X., Adamiec, A., Zhao, H., 2022. Critical role of the deep electron trap in explaining the inconsistency of sensitivity-corrected natural and regenerative growth curves of quartz OSL at high irradiation doses. Radiat. Meas. 159, 106874. https://doi.org/10.1016/j.radmeas.2022.106874.
- Poggemann, D.-W., Hathorne, E.C., Nürnberg, D., Frank, M., Bruhn, I., Reißig, S., Bahr, A., 2017. Rapid deglacial injection of nutrients into the tropical atlantic via antartic intermediate water. Earth Planet Sci. Lett. 463, 118–126. https://doi.org/ 10.1016/j.epsl.2017.01.
- Poggemann, D.-W., Nürnberg, D., Hathorne, E.C., Frank, M., Rath, W., Reißig, S., Bahr, A., 2018. Deglacial heat uptake by the southern ocean and rapid northward redistribution via antarctic intermediate water. Paleoceanogr. Paleoclimatol. 201, 103497. https://doi.org/10.1016/j.gloplacha.2021.103497.
- Portilho-Ramos, R.C., Chiessi, C.M., Zhang, Y., Mulitza, S., Kucera, M., Siccha, M., Paul, A., 2017. Coupling of equatorial Atlantic surface stratification to glacial shifts in the tropical rainbelt. Sci. Rep. 7, 1561. https://doi.org/10.1038/s41598-017-016/20-2
- Prasad, S., 2000. HF treatment for the isolation of fine grain quartz for luminescence dating. Ancient TL 18, 15–17.
- Reimer, P.J., Austin, W.E., Bard, E., Bayliss, A., Blackwell, P.G., Ramsey, C.B., et al., 2020. The IntCal20 Northern Hemisphere radiocarbon age calibration curve (0–55 cal kBP). Radiocarbon 62, 725–757. https://doi.org/10.1017/RDC.2020.41.
- Sawakuchi, A.O., Guedes, C.C., DeWitt, R., Giannini, P.C., Blair, M.W.N.J., Faleiro, F.M., 2012. Quartz OSL sensitivity as a proxy for storm activity on the southern Brazilian coast during the Late Holocene. Quat. Geochronol. 13, 92–102. https://doi.org/ 10.1016/j.quageo.2012.07.002.
- Sawakuchi, A.O., Jain, M., Mineli, T.D., Nogueira, L., Bertassoli, D.J., Häggi, C., Cunha, D.F., 2018. Luminescence of quartz and feldspar fingerprints provenance and correlates with the source area denudation in the Amazon River basin. Earth Planet Sci. Lett. 492, 152–162. https://doi.org/10.1016/j.epsl.2018.04.006.
- Sawakuchi, A.O., Rodrigues, F.C., Mineli, T.D., Mendes, V.R., Melo, D.B., Chiessi, C.M., Giannini, P.C., 2020. Optically stimulated luminescence sensitivity of quartz for provenance analysis. Methods Protoc. 3. 6. https://doi.org/10.3390/mps3010006.
- Schönfeld, J., Bahr, A., Bannert, B., Bayer, A.-S., Bayer, M., Beer, C., Garlichs, T., 2012. Surface and Intermediate Water Hydrography, Planktonic and Benthic Biota in the Caribbean Sea–Climate, Bio and Geosphere Linkages (OPOKA). Leitstelle Meteor, Institut für Meereskunde der Universität Hamburg [Meteor] Cruise No. 78, Leg 1 February 22–March 28, 2009, Colón (Panama)–Port of Spain (Trinidad and Tobago).
- Souza, P.E., Pupim, F.N., Mazoca, C.E., Río, I.d., Mineli, T.D., Rodrigues, F.C., Sawakuchi, A.O., 2023. Quartz OSL sensitivity from dating data for provenance analysis of pleistocene and holocene fluvial sediments from lowland Amazonia. Quat. Geochronol. 74, 101422. https://doi.org/10.1016/j.quageo.2023.101422.
- Tsukamoto, S., Nagashima, K., Murray, A.S., Tada, R., 2011. Variations in OSL components from quartz from Japan sea sediments and the possibility of reconstructing provenance. Quat. Int. 234, 182–189. https://doi.org/10.1016/j.guaint.2010.09.003.
- Wallinga, J., Murray, A.S., Bøtter-Jensen, L., Horowitz, Y.S., Oster, L., 2002.
 Measurement of the dose in quartz in the presence of feldspar contamination. Radiat.
 Protect. Dosim. 10, 367–370. https://doi.org/10.1093/oxfordjournals.rpd.a006003.
- Wang, X., Peng, J., Adamiec, G., 2021. Extending the age limit of quartz OSL dating of Chinese loess using a new multiple-aliquot regenerative-dose (MAR) protocol with carefully selected preheat conditions. Quat. Geochronol. 62, 101144. https://doi. org/10.1016/j.quageo.2020.101144.
- Zhang, J., Li, S.-H., Sun, J., Lü, T., Zhou, X., Hao, Q., 2023. Quartz luminescence sensitivity variation in the Chinese loess deposits: the potential role of wildfires. J. Quat. Sci. 38, 49–60. https://doi.org/10.1002/jqs.3462.
- Zhang, Y., Chiessi, C.M., Mulitza, S., Zabel, M., Trindade, R.I., Hollanda, M.H., Wefer, G., 2015. Origin of increased terrigenous supply to the NE South American continental margin during Heinrich stadial 1 and the younger Dryas. Earth Planet Sci. Lett. 432, 493–500. https://doi.org/10.1016/j.epsl.2015.09.054.